

Scaling and localization in fracture of disordered central-force spring lattices: Comparison with random damage percolation

I. Malakhovskiy* and M. A. J. Michels†

Group Polymer Physics, Technische Universiteit Eindhoven, P.O. Box 513, 5600 MB Eindhoven, The Netherlands

(Received 24 January 2006; revised manuscript received 29 May 2006; published 19 July 2006)

We analyze statistical and scaling properties of the fracture of two-dimensional (2D) central-force spring lattices with strong disorder by means of computer simulation. We run fracture simulations for two types of boundary conditions and compare the results both with the simulation of random damage percolation on the same lattices and with the analytical scaling relations of percolation theory. We investigate the scaling behavior of the macroscopic failure thresholds, the main features of the developing microscopic cluster statistics and damage pattern, and the roughness scaling of the final crack. Our observations show that simulated fracture has three clearly distinguished regimes. The initial phase displays short-range localization of damage, but it is soon replaced by a regime where damage develops in a uniform manner, qualitatively as in random percolation. Already before the maximum-stress point macroscopic localization and anisotropy come into play, resulting in final crack formation. The data of the second, uniform-damage regime can be fitted consistent with the scaling laws of random percolation. Beyond this regime a clear difference is observed with percolation theory and with earlier results from fuse-network models. Nevertheless, the final-crack roughness is found to scale accurately over at least three decades, with a roughness exponent consistent with limited available data for 2D systems and marginally consistent with the value for 2D percolation in a gradient.

DOI: [10.1103/PhysRevB.74.014206](https://doi.org/10.1103/PhysRevB.74.014206)

PACS number(s): 64.60.Ak, 62.20.Mk, 89.75.Da, 61.43.Bn

I. INTRODUCTION

Scaling or size dependence is of a great importance for any physical theory or experimental study. First of all, it reflects fundamental laws of the theory or real phenomena. Secondly, it has a direct practical meaning, showing how the behavior changes with system size. Scaling laws can be very different, but in the most simple and pure case, for theories and experimental observations with no characteristic length, scaling should have a form

$$S(L_2) \propto S(L_1) \left(\frac{L_2}{L_1} \right)^m, \quad (1)$$

where m is a scaling exponent.¹ This dependence represents how values of the physical quantity S for two different system sizes L_1 and L_2 are related.

The size effect in fracture was observed as early as in the 1500's by Leonardo da Vinci, who noticed that a short truss is stronger than a long one.¹ Later on it has been found experimentally for many materials that their strength decreases when the size of a sample is getting larger. The simplest explanation for this phenomenon would be the larger the sample, the larger the probability of finding a defect, and therefore the smaller the critical strain. In 1939 Weibull was the first to apply statistics in order to give the size effect a formal description.^{1,2} He discovered the importance of having a correct representation for the distribution of strengths of small material elements, in particular in the range of very low strength. Weibull introduced a function especially for this purpose, which is now known as the Weibull distribution. Most statistical theories of size effects that appeared later on were based on Weibull's concept.

Local heterogeneity is inevitable in any material, and the role of such disorder is crucial for fracture. Ideally homogeneous materials would have a fracture threshold many times

larger than real ones, would not have any size effect and there would be no reason for quasistatic-crack surfaces to be rough. Furthermore, microscopic disorder has a very strong influence on the macroscopic response of a material and can change it completely, from brittle to ductile, from elastic to plastic. Considering the extreme case of strong disorder is important, since it allows to make the effect of disorder really pronounced and also helps to understand to what extent the disorder is able to suppress typical features of materials deformation: localization and long-range interactions between local stress fields around single defects.

A second interesting and very intriguing experimental observation in fracture is the universal scaling of crack roughness.³ This reflects the dependence between the roughness (average height variation) Δh of a crack surface and the size d of the window over which it is calculated:

$$\Delta h = \langle \max\{h(y), y \in [y_0, y_0 + d]\} - \min\{h(y), y \in [y_0, y_0 + d]\} \rangle_{y_0}, \quad (2)$$

where y is the coordinate along the average crack-propagation direction and $h(y)$ is the height of the crack profile (Fig. 1).

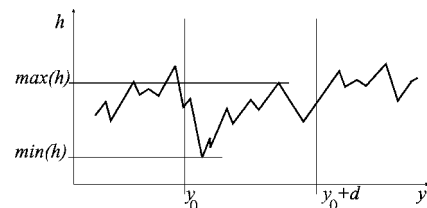


FIG. 1. Crack-roughness definition according to Eq. (2).

Surprisingly, for an extremely broad range of materials, with different properties and microstructure, the same scaling dependence

$$\Delta h \propto d^\zeta \quad (3)$$

has been found experimentally for the length scales up to a certain characteristic correlation length Ξ , after which the dependence saturates.³ Moreover, the value of the exponent ζ has been found to be nearly the same [about 0.8 for three-dimensional (3D) systems] for almost all investigated materials, while Ξ changes from one material to another. Although a lot of studies have been performed, there is no satisfactory explanation of this phenomenon so far.

Over the last decades rather significant efforts have been made to model deformation and fracture of heterogeneous materials by means of lattice (or “network”) models.^{4–15} First this approach has been applied to “fuse networks”—networks of resistors that are able to burn out at a certain critical load. The main focus of this research has been on such phenomena as threshold scaling, influence of the distribution of local properties on macroscopic behavior, and scaling of the damage-profile roughness. In most of the works fracture has been interpreted in terms of damage percolation. This approach has been based on a few important commonalities between the two phenomena. First of all, fracture of fuse networks and random percolation have one common object—the lattice. Secondly, disorder plays an important role for both, being an essential ingredient of fracture and the only driving force in random percolation. Scaling is the third common feature. In fracture experiments size scaling is observed for material strength and crack roughness. Percolation theory also reveals an intrinsic size effect. The internal structure of a large but finite cluster on a larger lattice shows self-similarity, and will become the percolating cluster when the lattice size decreases.

The fracture of lattices with moderate disorder or uniformly distributed properties is of course a highly correlated process, different from random percolation. However, the process of damage accumulation becomes less correlated with increasing disorder, and in the limit of infinite disorder it can be mapped onto a percolation problem.¹⁶ Still it is not clear to what extent strong, but finite disorder is able to make fracture statistically similar to percolation. If the answer is “yes”, it opens a way for percolation-theory arguments to be applied to fracture. If it is not the case, then another understanding of the underlying physics is needed.

A comparison between random percolation and fracture was already made in Ref. 12 on random 2D triangular lattices with central- and bond-bending forces and power-law disorder (see also Refs. 13 and 14 for more details). Based on a graphical representation of the force distributions in the network it was concluded that only the initial regime of damage development compared well with random percolation; the range over which this extended was observed to be significant only for strong disorder (a strong tail of very weak bonds), but to end well before the maximum in the curve of macroscopic stress vs strain. A detailed study for 2D central-force lattices⁶ has led to the view that for a very strong, but finite, power-law disorder, fuse networks behave similar to

percolating systems. For this special case fracture was found to belong to the same universality class as random percolation, and the exponent for threshold scaling coincided with percolation-theory predictions. However, the trend of the threshold scaling observed in Ref. 6 is different from random percolation: the rupture threshold decreases as the lattice size grows. In Ref. 6, even the exponent ζ for the scaling of crack roughness has been calculated, on the basis of percolation in a gradient, and was found to agree well with limited data on 2D systems.

The point of view of Ref. 6 has met rather serious opposition in Ref. 8. In that work the authors have also investigated fuse networks, but for a much larger size range, and significant deviations from the results of Ref. 6 and therefore from random-percolation theory, have been found. At the last fracture stage the authors have found localization in a form different from the observations of Ref. 6; they analyzed it in terms unrelated to percolation theory and demonstrated an accurate size scaling of the avalanchelike final breakdown event. The similarity to percolation was observed in Ref. 8 only at the early stage of the fracture process, but was not studied at the microscopic level or quantitatively confirmed. The two stages were believed to be separated by the maximum-stress point in the stress-strain curve and treated as unrelated.

The fuse-network model is anyway only a scalar analog of fracture. Even if all the features of fuse networks were known and thoroughly investigated and the question of (dis-)similarities between fuse networks and random percolation left no doubt, an attempt to associate fuse networks with fracture has an implicit weak point: mechanical deformation and therefore fracture of materials has a vectorial nature (it is described by a vectorial displacement field), while fuse-network simulations are based on conduction of current, which is described by a scalar potential field. In terms of lattice models it implies that each node (i.e., discretization point) has (in 2D) two degrees of freedom in the case of mechanical deformation and only one degree of freedom in the case of current conduction. Related to this, the central-force spring lattice allows for changes of its geometry during the deformation process, while in fuse-network simulations the geometry remains fixed. All mentioned features of the 2D central-force spring lattice imply that it should be a better model for deformation and fracture.

The main goal of the present research is to explore the origin of scaling in the fracture of disordered materials and, in particular, the possible connection with, and deviations from, percolation theory, with a mechanically more realistic model than fuse networks. To that end we have chosen central-force spring networks, simulated the macroscopic features and underlying microscopic statistics of fracture under uniaxial deformation, and compared the results with those of random percolation. In such a comparison, only theoretical predictions of percolation theory are usually involved.^{6,8} We performed numerical simulation of random percolation on the same lattices as used for fracture simulations, in order to see the detailed differences at all stages, so not only in the vicinity of percolation threshold, where the behavior of percolating lattices can also be assumed from scaling theory.

Very recently, the authors of Ref. 8 repeated their study also for 2D spring networks,⁹ although this time only for uniform disorder in the threshold distribution. Their conclusion is that with regard to the pattern of damage evolution and final fracture there are no essential differences between fuse networks and spring networks. But again, as in Ref. 8, no microscopic analysis of the percolationlike damage up to the point of maximum stress was attempted.

It should be realized that the theoretical threshold for random scalar percolation on regular triangular networks is 0.347.¹⁷ The threshold becomes 0.333 for percolation on the geometrically random networks chosen here.¹⁸ For elasticity percolation the value of the threshold is 0.641.¹² To have the thresholds for elasticity percolation and random scalar percolation equal we should have included bond-bending forces. However, for best comparison with the results of Refs. 6, 8, and 9 we have chosen central forces only; accordingly, we will not focus on the absolute threshold values in our results.

Our paper is organized in the following way. In Sec. II we describe the model (Sec. II A) and the methods, both for the simulation (Sec. II B) and for the analysis of the results (Sec. II C). Then in Sec. III we give the main results for two simulated phenomena: fracture and random percolation. We consider in particular the macroscopic features of mechanical behavior (Sec. III A) and finite-size scaling (Sec. III B), and the microscopic features of damage-cluster statistics (Sec. III C), damage anisotropy and localization (Sec. III D), and finally crack roughness (Sec. III E). For fracture we demonstrate an initial short-range localization phase, subsequent uniform damage development up to the point of maximum stress, and the onset of localization and anisotropy in the last stage of the fracture process. For random percolation of damage we check theoretical predictions on scaling. We compare the two phenomena both qualitatively and numerically, explicitly checking to which extent claims on percolation scaling in fracture are (or can be) true. We show the principal distinctions between the two phenomena, in the very beginning of the processes and beyond the maximum-stress point. For fracture we estimate the roughness-scaling exponent of the final crack, based on a direct analysis of spanning-cluster properties. In Sec. IV we discuss our general observations and finish with conclusions.

II. MODEL AND METHODS

The simulation scheme which we follow in the present research is the following. We first generate a spring network with a random geometry and locally varying properties, then run two types of simulation: the one of fracture and the one of random percolation (RP). After that the statistical analysis of results is performed. In Table I the statistics of the simulation runs is presented.

A. Lattice and boundary conditions

In our study we consider 2D lattices of central-force springs. The geometry of the lattice is random and is built as a Delaunay tessellation (a set of lines connecting each node to its natural neighbors, see, e.g., Ref. 19) of a square region

TABLE I. Statistics of simulation runs.

Linear lattice size L (2D)	Number of runs
12	500
17	500
25	500
35	150
50	100
70	30
100	20
150	10
200	5

with randomly distributed nodes (Fig. 2). Note that the average coordination number of an infinite Delaunay tessellation is always 6, while the local number may vary from 3 to infinity; due to the boundaries our average coordination number is very close to 6, ensuring mechanical rigidity of the intact network.

Obviously one does not need any loading boundary conditions (BC's) for the simulation of RP, but they are necessary for the simulation of deformation and fracture. In this work we apply two types of boundary conditions: "busbars" and periodic. In the first case a uniaxial tensile strain is imposed by means of two rigid busbars at the left and right sides of the lattice, while the upper and lower boundaries remain free:

$$u_x(0,y) = 0, \quad u_x(1,y) = U, \quad u_x(0,0) = u_y(0,0) = 0, \quad (4)$$

where u_x, u_y are the displacements along x and y axes, respectively, with coordinates x, y each in the unit interval $(0,1)$ and where U is the prescribed displacement.

In the second case the strain is applied to the lattice via imposing equal relative displacement to the opposite nodes at the left and right sides of the lattice. The opposite nodes of the upper and lower sides are also restricted to have equal relative displacement, which is defined by the solution as an independent degree of freedom:

$$u_x(1,y) - u_x(0,y) = U, \quad u_y(1,y) = u_y(0,y),$$

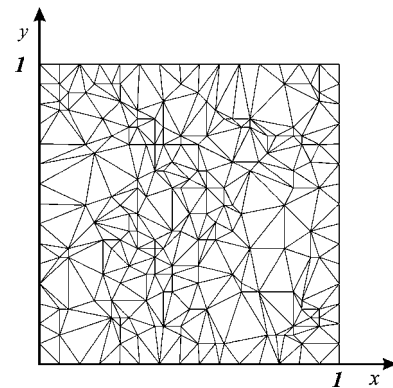


FIG. 2. Example of a Delaunay-tessellation lattice ($L=15$) as used in the simulations.

$$u_y(x,1) - u_y(x,0) = V, \quad u_x(x,1) = u_x(x,0),$$

$$u_x(0,0) = u_y(0,0) = 0, \quad (5)$$

where u_x, u_y are again the displacements along x and y axes, U is the prescribed horizontal displacement and V is the vertical displacement, which remains an independent degree of freedom. In this case the shape of the deformed opposite sides always stays identical, as if the lattice were wrapped around a torus. This type of loading is used to eliminate the influence of boundaries.

B. Simulation methods

In the case of RP simulation, lattice bonds are randomly removed from the lattice one by one. The result of this simulation is nothing more than a random sequence of removed bonds, without any correlation or underlying physics. The simulation of fracture is of course different. Upon loading, each bond behaves first as an elastic spring and as the threshold strain is reached the bond breaks (it is irreversibly removed from the lattice).

In order to simulate strong disorder, the strain thresholds t of individual bonds are randomly generated according to the following distribution:

$$P(t) = (1 - \alpha)w^{\alpha-1}t^{-\alpha}, \quad t \in [0, w], \quad (6)$$

while Young's modulus remains the same for all bonds. So there is an algebraically diverging tail of very weak bonds.

A finite-element problem is formulated and solved for a given set of boundary conditions in order to determine the spring with the highest ratio of actual strain to threshold. If the highest ratio is more than or equal to 1, the corresponding spring is removed from the lattice and the finite-element problem is solved again for the modified lattice, until no break events occur for the given boundary conditions. Thus, the stiffness matrix is modified and equations are resolved every time a spring breaks. Bonds are allowed to be broken only one by one. Removing the broken bond is done for calculational reasons by putting its stiffness equal to a very small positive value, i.e., to almost zero.

Technically the fracture part of our model is an iterative finite-element model, consisting of breakable central-force springs with random properties. The stiffness matrix is fully assembled and constrained according to boundary conditions only once (in the beginning) and after that it is only modified when any bond breaks. The obtained system of linear algebraic equations is solved as many times as breaking events occur until the boundary conditions are satisfied or the system falls apart.

Calculations are performed for a range of lattice sizes from $L=12$ to $L=200$ and for a set of samples per size (from 500 to 5, depending on size) in order to get sufficient statistical information. The results presented in this paper have been obtained for the particular case of "strong disorder," governed by the threshold distribution (6) with $\alpha=0.7$. Although the disorder would be stronger for α closer to 1, the value 0.7 provides a reasonable compromise whereby the disorder is strong enough, but the problem is still not com-

putationally too demanding. In the mentioned studies^{6,8,9} the same general power-law threshold distribution (6) was used, with disorder exponents $\alpha=9/10$ and $\alpha=2/3$,⁶ $\alpha=19/20$ and $\alpha=0$ (i.e., uniform disorder),⁸ and $\alpha=0$.⁹

C. Methods for the analysis of results

We obtain two types of results in our simulation: mechanical and statistical ones. The mechanical responses of the lattices (or stress-strain relationships) are calculated directly and rather easily from the reaction forces. This is the analog of data that would result from real fracture experiments. Statistical results of course require some processing. The methods we use in this paper to analyze them are mostly taken over from percolation theory^{17,20} and simulation.

From the macroscopic stress-strain curves we calculate two important properties: the survival probability P_{surv} —the probability that a lattice survives (remains unbroken) at a certain density p of broken (removed) bonds—and the critical strain ε —the strain at which the stress reaches its maximum and the lattice starts breaking. An effective threshold p_{50} —the density at which 50% of lattices survive—can be obtained from P_{surv} .

By analyzing the damage patterns we identify clusters of connected broken (removed) bonds and calculate the following set of microscopic cluster properties as functions of p —the density of broken (removed) bonds.

The cluster-size distribution n_s (the number of clusters of weight s divided by the total number of sites in the lattice), together with the weight-averaged cluster size

$$S = \frac{M_2}{M_1} = \frac{\sum_s n_s s^2}{\sum_s n_s s}, \quad (7)$$

describing the statistics of damage clusters ($M_1=p$ and M_2 are the first and the second moment of the cluster-size distribution, respectively).

The average squared gyration radius R_s , showing the spatial extent of clusters of a particular weight s :

$$R_s^2 = \left\langle \frac{\sum_{i=1}^s |\mathbf{r}_i - \mathbf{r}_{\text{c.m.}}|^2}{s} \right\rangle_{\text{(all } s\text{-clusters)}}, \quad (8)$$

where $\mathbf{r}_{\text{c.m.}}$ is the center-of-mass of an individual cluster and \mathbf{r}_i defines the location of each cluster node.

The correlation length ξ , which is an average distance between two sites of the same cluster

$$\xi^2 = \frac{2 \sum_s R_s^2 s^2 n_s}{\sum_s s^2 n_s}. \quad (9)$$

In order to identify possible anisotropy of the developing fracture pattern we also calculate longitudinal and transversal correlation lengths

$$\xi_{\parallel}^2 = \frac{2 \sum_s X_s^2 s^2 n_s}{\sum_s s^2 n_s}, \quad \xi_{\perp}^2 = \frac{2 \sum_s Y_s^2 s^2 n_s}{\sum_s s^2 n_s}, \quad (10)$$

where X_s, Y_s are defined similar to the gyration radius

$$X_s^2 = \left\langle \sum_{i=1}^s \frac{|x_i - x_{c.m.}|^2}{s} \right\rangle_{\text{(all } s\text{-clusters)}},$$

$$Y_s^2 = \left\langle \sum_{i=1}^s \frac{|y_i - y_{c.m.}|^2}{s} \right\rangle_{\text{(all } s\text{-clusters)}}, \quad (11)$$

with $x_{c.m.}, y_{c.m.}$ denoting the coordinates of the center-of-mass and x_i, y_i being the coordinates of cluster nodes. From Eq. (10) a shape factor can be defined as

$$\Phi = \frac{\xi_{\perp} - \xi_{\parallel}}{\xi_{\perp} + \xi_{\parallel}}, \quad (12)$$

describing the damage anisotropy.

In the case of random damage, percolation theory describes the large-scale statistics of the developing cluster distribution and cluster pattern, when local details in the underlying lattice become irrelevant. In particular it predicts then the following universal scaling laws for an infinite lattice in the vicinity of the percolation threshold p_c :^{17,20}

$$S \propto M_2 \propto |p - p_c|^{-\gamma}, \quad (13)$$

$$\xi \propto |p - p_c|^{-\nu}, \quad (14)$$

$$n_s \propto p s^{-\tau} f(s^{3-\tau}/S), \quad (15)$$

$$R_s \propto s^{1/D_f}, \quad (16)$$

where f is a scaling function and where the exponents take universal values depending only on dimension D and obeying the following relations:

$$\frac{D_f}{D} = \frac{1}{\tau - 1}, \quad \frac{\gamma}{\nu D} = \frac{3 - \tau}{\tau - 1}. \quad (17)$$

For $D=2$ one has $\gamma=43/18$, $\nu=4/3$, $D_f=91/48$, $\tau=187/91$, while p_c and all the proportionality factors depend on lattice details. The scaling function $f(z)$ should approach a constant for $z \ll 1$ and decrease to zero for $z \gg 1$.

In practice, of course, only finite-size lattices are considered. For a finite system, ξ approaches the lattice size at an effective threshold when a spanning cluster appears. For a series of finite-size samples p_{50} is a natural estimate of the average threshold. Substituting $\xi=L$, $p=p_{50}$ into Eq. (14) results in the finite-size scaling relationship for the percolation threshold

$$p_{50} = p_c - \frac{c}{L^{1/\nu}}, \quad (18)$$

where c is a constant. Finite-size scaling also adds an extra proportionality factor in form of $\phi(\frac{L}{\xi})$ to the expressions (13)–(16).

By checking the validity of the above expressions for our simulation results we can find out to what extent the simulated fracture process resembles random percolation of damage. While in RP damage develops isotropically and the spanning cluster looks similar to a cloud rather than a crack, in our fracture simulation the crack and the corresponding

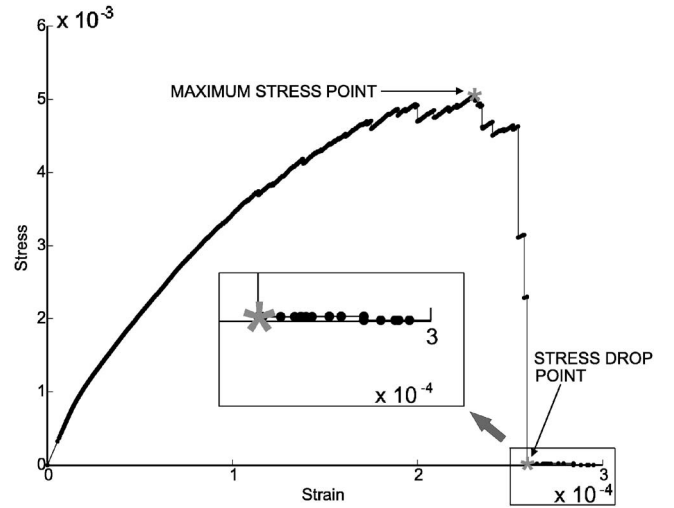


FIG. 3. Stress-strain relationship (dots represent breaking events) for a single fracture simulation ($L=200$).

spanning cluster of broken bonds is easily identified as a localized and anisotropic object elongated perpendicular to the applied load. The roughness Δh in the loading direction x can subsequently be calculated according to Eq. (2) as a function of the window length d in the perpendicular direction y , whereupon the roughness scaling exponent ζ is obtained as a result of least-squares fitting.

A way of estimating the roughness scaling exponent directly from percolation theory was suggested by Hansen and Schmittbuhl, who used the concept of percolation in a gradient.⁶ They argue that at breakdown the damage density $\langle p \rangle$ averaged in the direction perpendicular to the loading on the one hand satisfies $\langle p \rangle - p_c \propto \xi^{-1/\nu}$ and, on the other hand, $\langle p \rangle - p_c \propto (h/L)^2$ (a symmetric damage profile, with h the coordinate in the loading direction). Subsequently assuming that the final roughness Δh is reached around $h=\xi$, they thus derive

$$\Delta h \propto L^{\zeta}, \quad \zeta = \frac{2\nu}{1 + 2\nu}. \quad (19)$$

The use of this method for fuse networks is based on the applicability of the arguments of percolation in a gradient and on the RP-like scaling of ξ in this case. With the RP value $\nu=4/3$ in 2D it leads to the value $\zeta=8/11=0.73$ for the roughness exponent.

III. RESULTS

Macroscopically the fracture process in our model has some features very typical for highly disordered systems. With the chosen strong disorder there is no linear-elastic part in the stress-strain dependence; the stress-strain curve for one particular lattice with size $L=200$ is shown in Fig. 3. Weak springs start breaking from the very beginning, decreasing the overall stiffness and bending the stress-strain curve downwards. This is very much different from the well-known “weakest link” concept, according to which global failure develops as an avalanche right after the failure of a

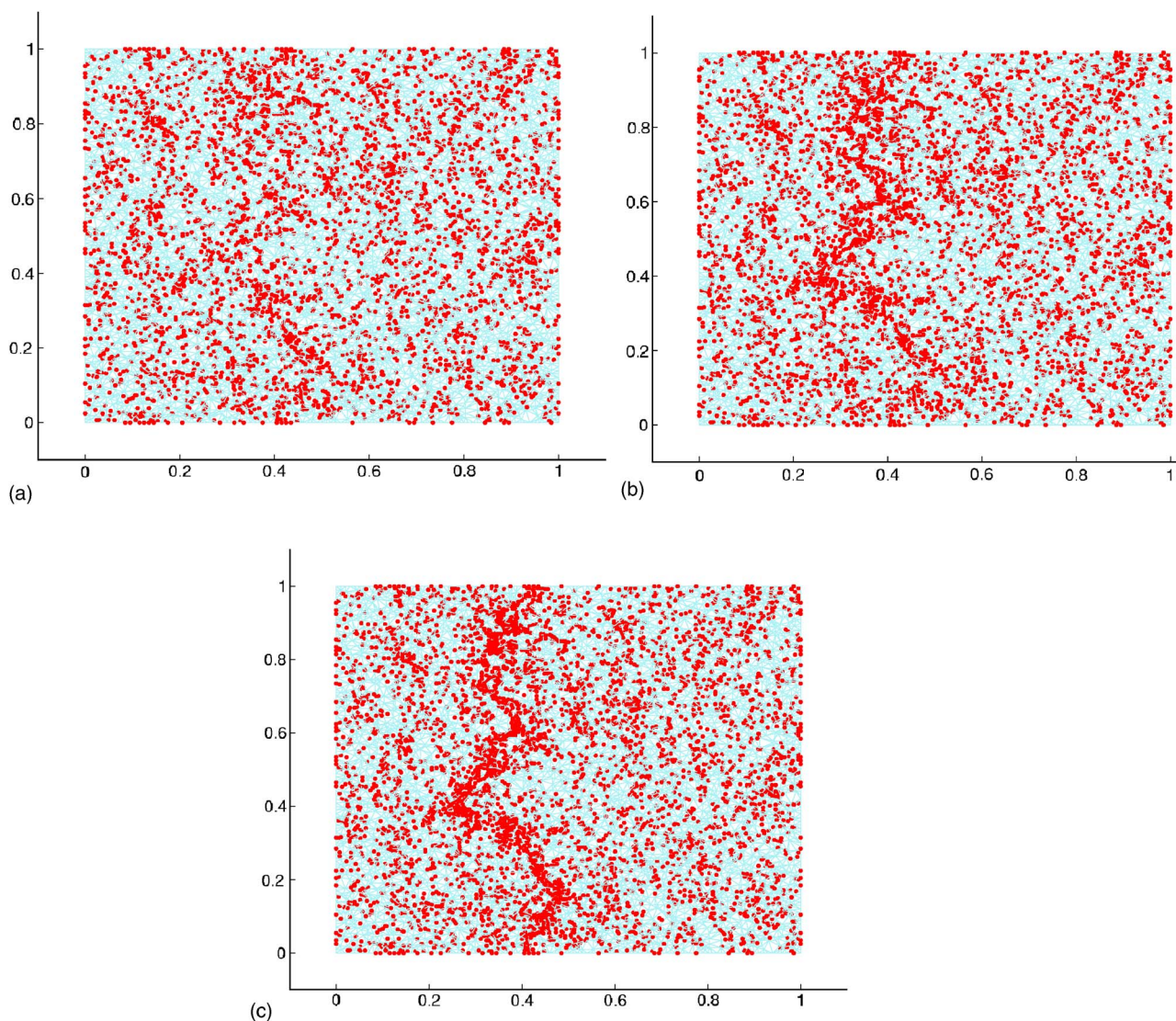


FIG. 4. (Color online) Developing damage pattern in a single fracture simulation with lattice linear size $L=100$ (red/dark gray dots represent the centers of broken bonds): maximum-stress point with main-crack appearance (a), main-crack growth (b), and broken lattice (c).

few weakest bonds. In our case the lattice starts breaking apart after a rather long quasielastic regime.

In our simulations the two types of boundary conditions give qualitatively identical results with very close values of fit parameters. The only significant numerical difference was observed for the values of the macroscopic critical stress and strain, which appear to be higher for busbars boundary conditions. Therefore, only results for periodic boundary conditions are presented graphically in the present section, while the numbers are given for both.

For RP the criterion for identifying when the lattice is broken is obvious: at the point of the first spanning-cluster formation. On the contrary, in fracture simulation we can identify at least two characteristic points on a stress-strain curve: the point of maximum stress and the point where stress drops down to zero or almost zero. The first point precedes fracture and the second one is the mechanical breakdown itself. On top of that there is a final point at which the first spanning cluster is formed—the percolation threshold in the ordinary sense. So note that the percolation thresh-

old and the mechanical breakdown are not necessarily identical: the former is defined according to topological connectivity, while the latter has to do with rigidity.

When the microscopic damage is considered, our simulations show that during the initial phase of fracture short-range localization takes place. However, this is rather soon suppressed by disorder. Then coarse-grained damage develops in a distributed way, but already before the maximum-stress point it is possible to see the beginning of macroscopic localization. Beyond the maximum-stress point this localization develops further, along with a steep stiffness decrease, until finally a spanning crack is formed (Fig. 4). The full damage development happens in the same way for both types of applied boundary conditions. The observations suggest that if there is a similarity between fracture in our model and RP it is only expected to occur after the end of the initial short-range localization phase and well before the point of maximum stress. The stress-drop point, representing mechanical breakdown, is far beyond the expected percolation-like regime. This implies that the study of the 50% survival

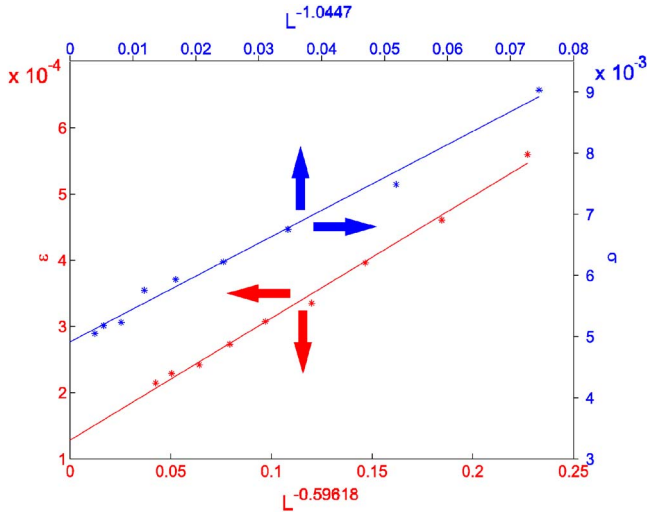


FIG. 5. (Color online) Size scaling of the macroscopic critical stress σ (upper curve) and strain ε (lower curve) according to the maximum-stress criterion for fracture with periodic boundary conditions; drawn lines correspond to least-squares fitting.

probability for fracture (in particular with the stress-drop point taken as the point of failure, but probably also with the maximum-stress point) in terms of RP is then doubtful due to the fact that in this measure both lattices inside and outside of the regime of distributed damage are taken into account.

A. Macroscopic critical stress and strain

The macroscopic critical stress σ and critical strain ε are defined for each sample as the maximum stress and the corresponding strain, respectively. The values of σ and ε are averaged over a set of samples for each system size. Similar to experimental observations, the critical stress and strain decrease as the size of the lattice becomes larger, due to disorder. The size dependence of the macroscopic critical stress follows a power law $\sigma - \sigma_\infty \propto L^{-\kappa}$ for both types of boundary conditions, with $\kappa=1.04$, $\sigma_\infty=4.9 \times 10^{-3}$ for periodic BC's (Fig. 5) and $\kappa=0.97$, $\sigma_\infty=1.3 \times 10^{-2}$ for busbars. The critical strain follows the same behavior $\varepsilon - \varepsilon_\infty \propto L^{-\lambda}$, but with different numbers $\lambda=0.60$, $\varepsilon_\infty=1.3 \times 10^{-4}$ for periodic BC's (Fig. 5) and $\lambda=0.59$, $\varepsilon_\infty=2.2 \times 10^{-4}$ for busbars. Apparently the exponents are independent of boundary conditions within the considered data accuracy $\lambda \approx 0.6$, $\kappa \approx 1$, while the absolute values of ε and σ are significantly higher for the busbars case.

B. Finite-size scaling

As has been already mentioned, random percolation on a lattice must reveal finite-size scaling in the form (18) with a proper threshold and a scaling exponent. For our simulation of RP we have checked this scaling law by collapsing the survival-probability plots for different lattice sizes (not shown). Scaling in the form of $p_{50} - p_c \propto L^{-1/\nu}$, with $\nu=4/3$ as predicted by theory, and $p_c=0.3333$ as given in Ref. 18 for random lattices, matches our results very well. Contrary to that, the data for fracture cannot be fitted to Eq. (18) with the

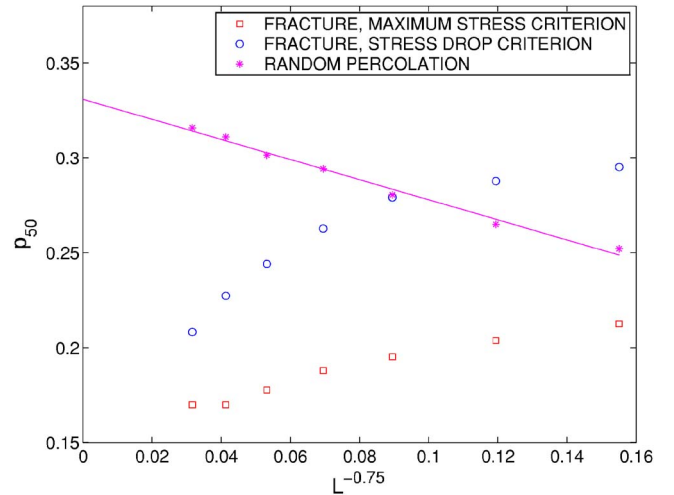


FIG. 6. (Color online) Size dependence of the effective threshold p_{50} , scaled with the theoretical exponent $\nu=4/3$ of RP, for random percolation and fracture with periodic boundary conditions.

theoretical values. It is clearly seen (Fig. 6) that the graph corresponding to the stress-drop criterion has a significant curvature when scaled with the exponent of $4/3$. The graph following from the criterion of maximum stress does not look straight either, although the deviations are not as dramatic. Furthermore, the data corresponding to fracture simulation show a decrease of p_{50} with increasing lattice size, while RP simulation gives an opposite dependence. A similar contradiction for fuse networks, although not noticed, can be found in the results of Ref. 6, while the scaling exponent is found there to coincide with percolation theory.

Both fracture curves in Fig. 6 get straighter with increasing scaling exponent, as was also observed in Ref. 8. For the periodic BC's and the maximum-stress criterion, the values of the exponent and threshold that provide the straightest p_{50} graphs and the best collapse of survival probability plots, are $p_c=0.14$, $\nu=2.24$ (Fig. 7). If the criterion of "broken lattice" is taken according to stress drop, the values become $p_c=0.05$, $\nu=4.57$, but with less fitting quality. These numbers are the result of nonlinear fitting of p_{50} , which allows one to obtain ν and p_c together.

The observations for the option with busbars boundary conditions give, within this accuracy, the same values for p_c and ν for the maximum-stress criterion, and slightly different ones if the criterion of stress drop is chosen: $p_c=0.08$, $\nu=3.72$.

The above results show that for a real fracture simulation the size dependence can be made to fit at least approximately a power-law scaling, but with parameters much different from those valid for RP and found in Ref. 6. However, as mentioned already, the very nature of the survival distribution implies that here data without and with a strong macroscopic localization have been combined in one analysis; without further study of the localization regime no conclusions should be attempted from such deviating power-law scaling, except that there is a clear difference with earlier results for fuse-network models that suggest a quantitative agreement with RP up to the final failure point.⁶

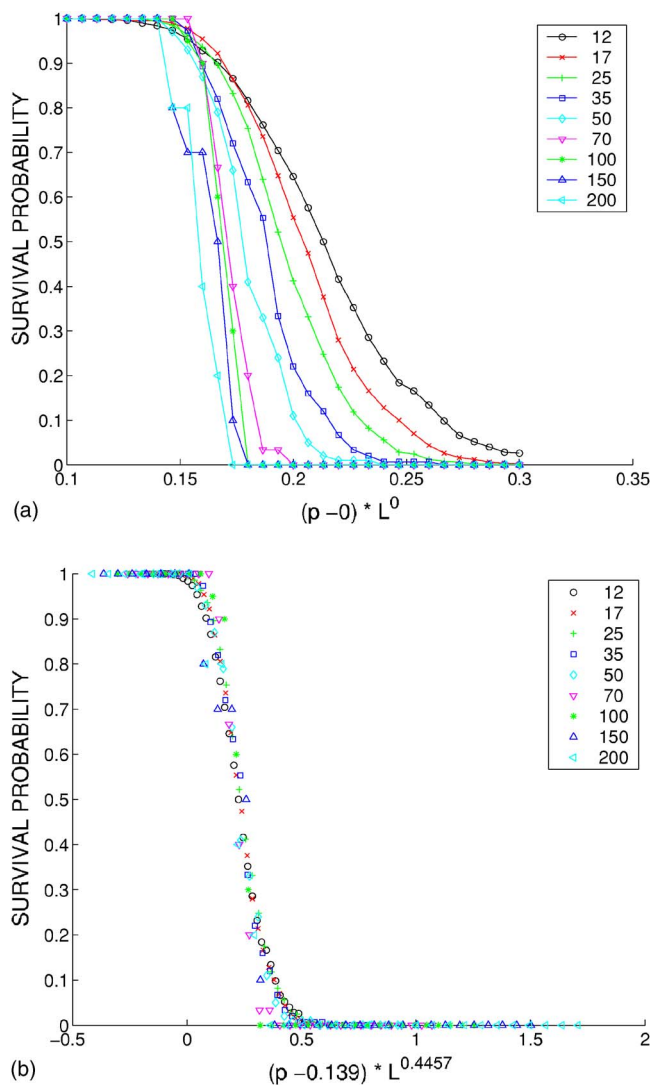


FIG. 7. (Color online) Survival probability for fracture simulation with periodic boundary conditions and the maximum-stress criterion: not scaled (a) and scaled with a power law for $p-p_c$ according to the best least-squares fit of p_{50} (b).

C. Cluster statistics

We have taken lattices of one particular size $L=50$ and analyzed the average behavior of the distribution n_s of damage-cluster sizes. Figure 8 gives the full distribution for RP (upper part) and fracture (lower part). For RP the power-law scaling at the approach of p_c is recognized, with the correct value of the Fisher exponent $\tau=187/91$. A qualitatively similar scaling is suggested for fracture, though in a smaller range of p . To accurately plot the scaling according to percolation theory, we have replotted the data in the form of Eq. (15), see Fig. 9. The requirement that the scaling function $f(z)$ has a plateau for $z \rightarrow 0$ then proves a fairly sensitive test to the value of τ . Although a slight shape difference exists between the scaling functions for RP and fracture, it has to be concluded that in the considered interval of p (i.e., before the macroscopic localization occurs) the fracture data are consistent with the scaling law (15) and the exponent value $\tau=187/91$ of random damage percolation.

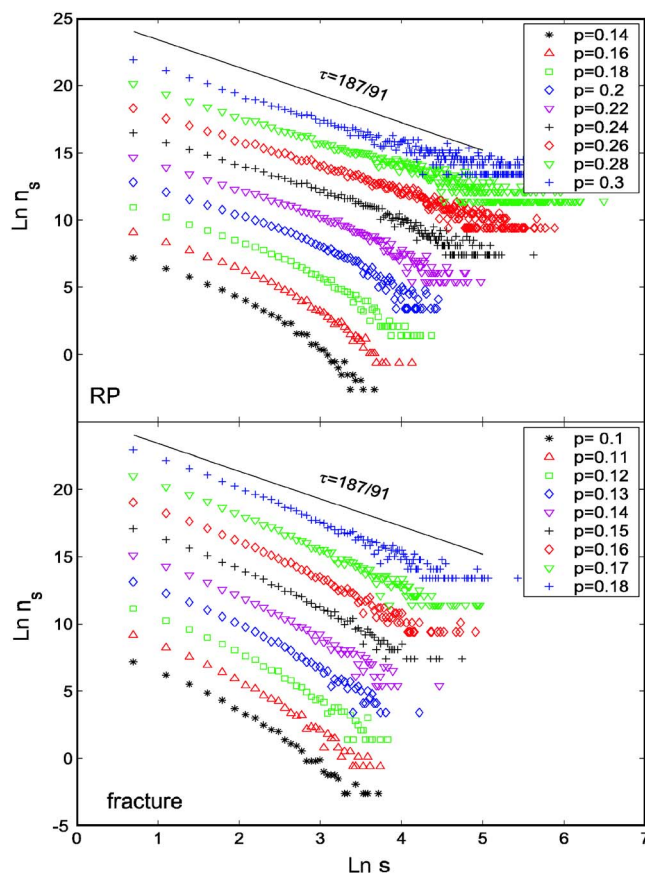


FIG. 8. (Color online) Cluster-size distribution for random percolation (upper graph) and fracture (lower graph) simulations. The data represent averages over all samples of size $L=50$. The solid lines show the theoretical RP slope on approach of p_c .

Following this conclusion we can also verify the additional scaling laws (13) and (14) vs distance to p_c , for the second moment M_2 of the mass distribution and for the spatial correlation length ξ , respectively. As seen from the graphs (Figs. 10 and 11) the second moment M_2 of the cluster-size distribution as well as the correlation length ξ do not develop in the same way for RP and for fracture simulation. In the case of fracture the cluster mass and cluster extent on average progress faster with damage concentration p . There is a difference in the initial regime, especially well observed for ξ ; snapshots of the damage suggest that this is related to an initial enhanced fracture of springs oriented parallel to the loading direction, and to short-range localized growth of the initial fractures. Also the anisotropy and macroscopic localization that in fracture set in around the maximum-stress point, cause visible difference from RP behavior. However, in the intermediate regime, at concentrations corresponding with the scaling in Fig. 9, the fracture data for M_2 and ξ can be consistently fitted to the RP scaling laws and exponents. The extrapolated fracture percolation threshold $p_c=0.27$ is well below that of RP ($p_c=0.33$). Note that the fracture data in which scaling can be observed are in relative terms still farther from p_c than those for RP; this is again consistent with the cluster-size statistics of Fig. 8, in which the range of algebraic scaling remains smaller for fracture.

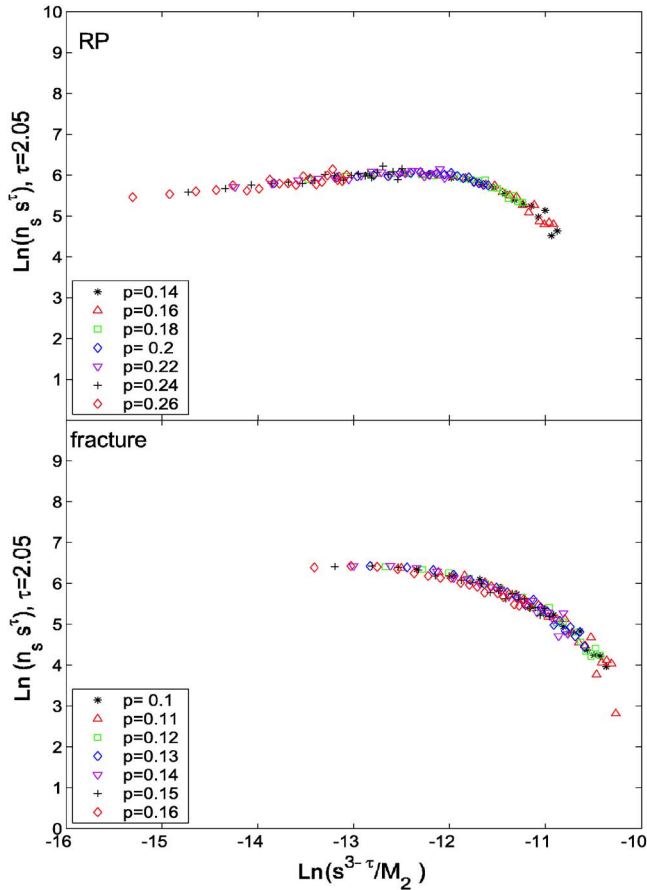


FIG. 9. (Color online) Scaling function of the cluster-size distribution for RP (upper graph) and fracture (lower graph) simulation within the scaling regime. The data represent averages over all samples of size $L=50$; scattered data for large s are excluded; curves are leveled vertically to match one another [see Eq. (15)].

The above picture of three regimes, with accelerated cluster growth in the initial and final stages, and with intermediate RP statistics, is supported by Fig. 12; here we have plotted as a function of increasing damage the joining probability—the probability for an individual newly broken bond to be joined to an already existing damage cluster instead of nucleating a new cluster of one bond.

The relationship between the cluster size (weight) s and the cluster spatial extent R_s for big clusters defines the fractal dimension D_f . Figure 13 again shows for a damage concentration inside the scaling regime ($p=0.14$) that fracture and RP data match, with the correct theoretical value $D_f = 91/48$. This observation further supports the statement that there is a regime in fracture that matches the scaling relations of RP.

D. Damage anisotropy and localization

The final damage patterns are completely different for RP and fracture. For the former case one sees several big isotropic damage clusters, one of which spans through the lattice [Fig. 14(a)]. In the case of fracture, anisotropy of a final damage pattern can be easily noticed by the naked eye [Fig.

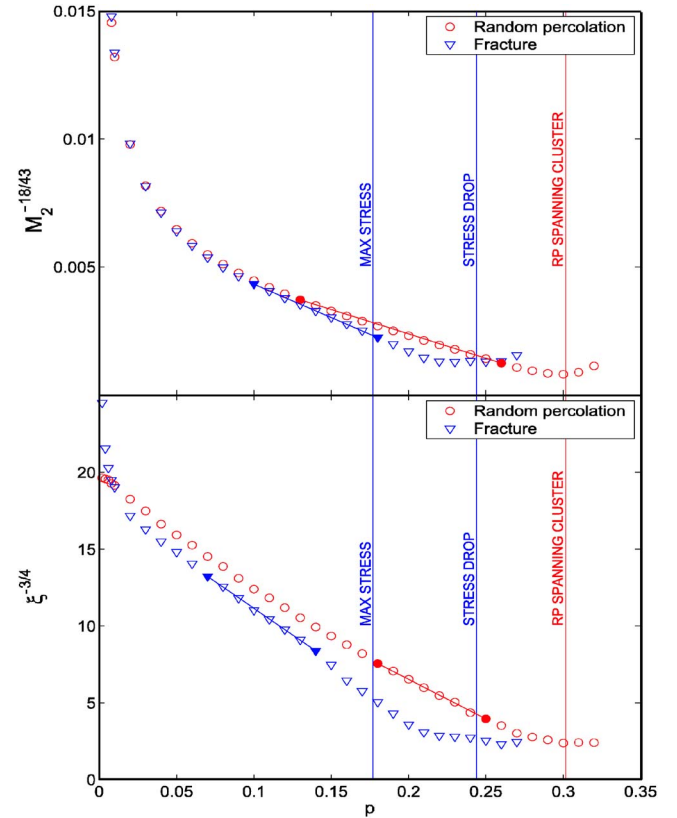


FIG. 10. (Color online) Scaling of the second moment M_2 of the cluster-size distribution (upper graph) and scaling of the correlation length ξ (lower graph) for simulations with linear lattice size $L = 50$. Limits of the scaling regime are denoted by solid markers; the straight solid lines show the theoretical RP slopes on approach of p_c .

14(c)]. It is also seen that the biggest fracture cluster is far larger than any other, suggesting that the damage pattern is localized; the damage pattern at the point of maximum stress still remains rather isotropic and does not reveal pronounced localization, although the major cluster has been nucleated by this moment [Fig. 14(b)].

Anisotropy can be observed quantitatively by monitoring the shape factor Φ constructed from the two components $\xi_{||}$, ξ_{\perp} of the correlation length, and defined by Eq. (12); here we take spanning clusters into account together with others, while in the scaling analysis of M_2 and ξ spanning clusters are always excluded from consideration. For an uncorrelated and delocalized process Φ should obviously remain statistically equal to zero for any density of broken bonds. Although the shape factor corresponding to fracture has a stable non-zero level from the very beginning, it starts to deviate from zero significantly only slightly before the point of maximum stress and grows dramatically beyond the maximum stress (Fig. 15). This results in a final ratio of the components of the correlation length of about three. Hence the fracture process gains two clear principal features just before the maximum-stress point: damage anisotropy and localization.

E. Roughness scaling

Damage clusters forming in RP simulation are isotropic, and the largest one is not much larger than others. Therefore

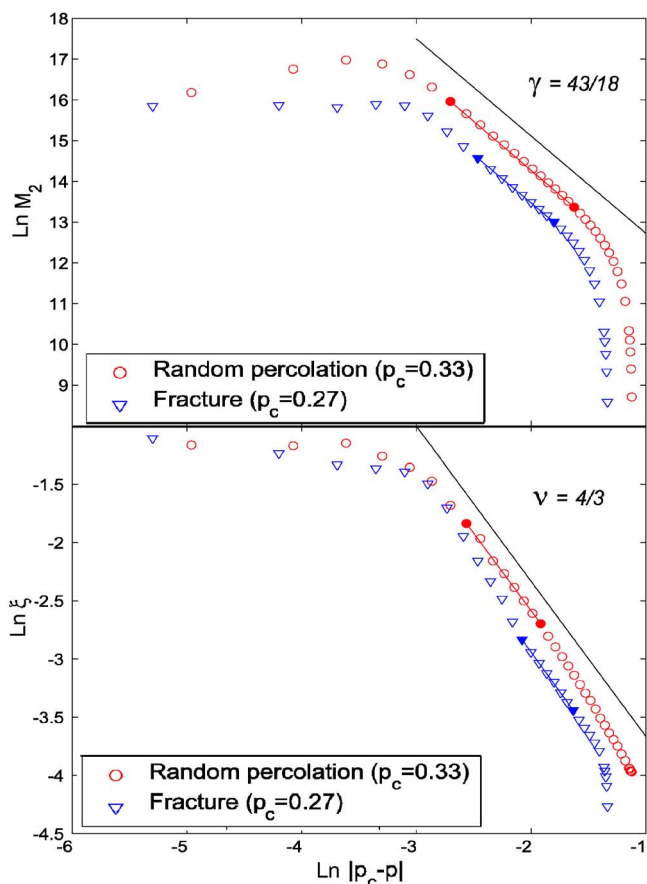


FIG. 11. (Color online) Scaling of the second moment M_2 of the cluster-size distribution (upper graph) and scaling of the correlation length ξ (lower graph) as functions of $|p_c - p|$ for simulations with linear lattice size $L=50$. Limits of the scaling regime are denoted by solid markers; the black solid lines show the theoretical RP slopes.

it is impossible to recognize a cluster that looks similar to a crack. Contrary to this, in our fracture simulation it is always possible to identify the dominant final damage cluster that contains a path connecting opposite sides of the lattice, i.e., the crack. The obvious question then is whether the roughness of this crack scales as like it does in experimental observations.

In order to obtain the crack profile as a function of the transversal coordinate, we average in the direction of applied strain the coordinates of bonds of the heaviest damage cluster of an individual lattice (Fig. 16). Subsequently we calculate the roughness scaling exponent of the obtained profile, using Eq. (2), by least-squares fitting. This procedure is performed for all samples with $L \geq 70$. The data collapse onto a straight line on a log-log plot remarkably well (Fig. 17), giving very close values of the scaling exponent for different samples and different lattice sizes. It is indeed surprising to find such a pronounced scaling law at a stage far beyond the scaling range of RP-like damage. The scaling exponent, averaged over all considered samples, is $\zeta = 0.65 \pm 0.07$.

The above procedure of averaging in the horizontal direction of loading to get the position of the crack, is in line with the way in which the horizontal fluctuation of the crack position is described in the original paper⁶ in terms of damage

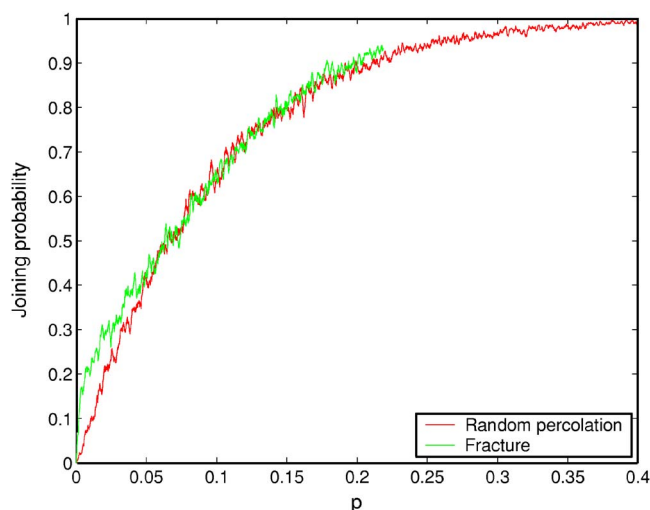


FIG. 12. (Color online) Joining probability (the probability for an individual newly broken bond to be joined to an already existing damage cluster) for simulations with linear lattice size $L=50$ for RP (red or dark gray) and fracture simulation (green or light gray). The curves are smoothed by a moving average over ten subsequent points.

correlations in gradient percolation, and taken there as a basis for the roughness scaling. However, this is a rather vague way of defining the real-crack roughness, and as an alternative we can choose the backbone of the infinite cluster, however, with at least one important caveat. The infinite cluster may have loops, leading to nonunique crack paths in the backbone, and possibly also vertical overhangs. Comparison with real cracks is then probably only meaningful on a length scale larger than the typical local width of the infinite cluster, i.e., the depth of the subsurface damage. We have used the burning algorithm²¹ to determine the infinite backbone clusters of our simulations, and analyzed their roughness scaling. Taking all length scales into account we then find a rough-

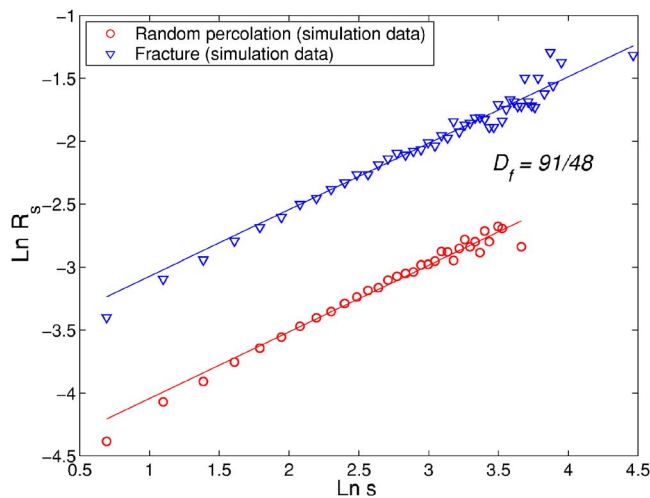


FIG. 13. (Color online) Relationship between the cluster weight s and the cluster gyration radius R_s at the density of broken bonds $p=0.14$ for $L=50$. The data for fracture are shifted one unit up. Solid lines show the theoretical RP value of the fractal dimension.

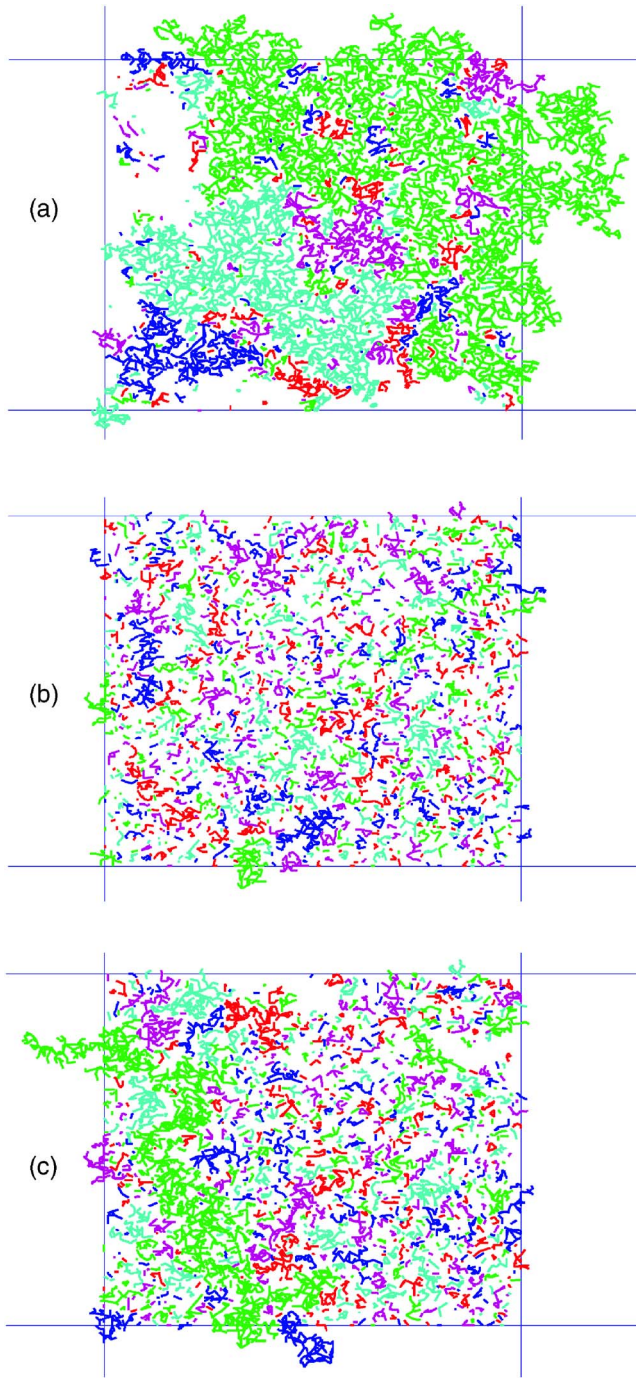


FIG. 14. (Color online) Clusters of broken bonds for a single lattice with linear size $L=100$. (a) For RP simulation at the threshold, (b) for fracture simulation at the maximum-stress point, and (c) for fracture simulation at the stress-drop point.

ness exponent $\zeta=0.81\pm 0.06$, somewhat higher than the above result from horizontal damage averaging. Eliminating the lower length scales we see as expected that the roughness changes, and get $\zeta=0.74\pm 0.11$; this is statistically sufficiently close to our averaging value, which hardly changes when lower lengths are ignored: $\zeta=0.67\pm 0.12$.

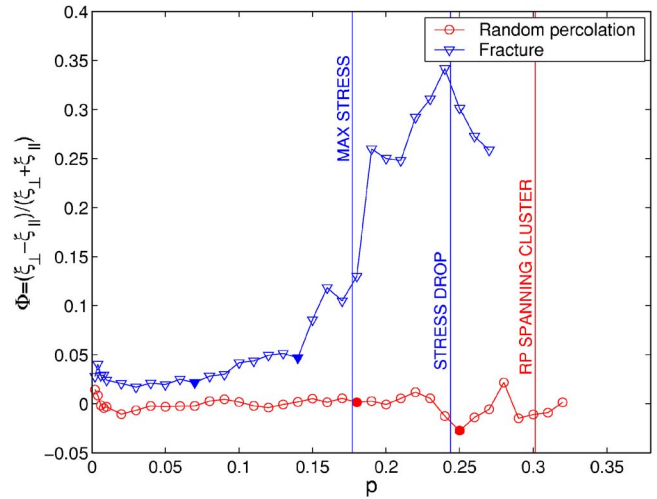


FIG. 15. (Color online) Shape factor Φ of damage clusters for fracture and RP. The data represent averages over all samples of size $L=50$. Markers indicate the regime where in Figs. 10 and 11 the correlation length ξ is shown to numerically obey RP scaling.

IV. DISCUSSION AND CONCLUSIONS

The work reported in this paper is an attempt to understand similarities and distinctions between fracture of central-force spring lattices and random percolation, both on macroscopic and microscopic levels, by elaborating the statistical and scaling features of the two phenomena.

The fracture scenario of our model is very typical for highly disordered systems: break events start to occur from the earliest stage of deformation, but do not lead to macroscopic failure until, after progressive distributed damage, the system reaches its critical state. This behavior is different from the way fracture happens in nondisordered or weakly disordered systems, where failure develops as an avalanche already after only few break events.

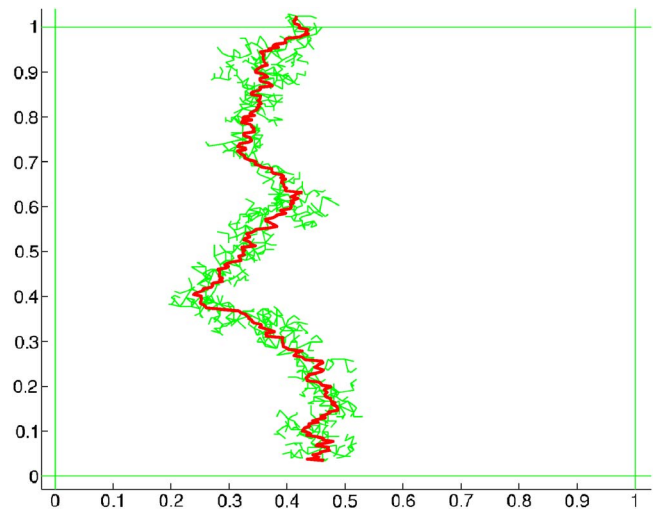


FIG. 16. (Color online) Example of a crack profile (red or dark gray line) obtained from the biggest damage cluster (green or light gray) for a single simulation with $L=100$ by averaging in the direction of applied load.

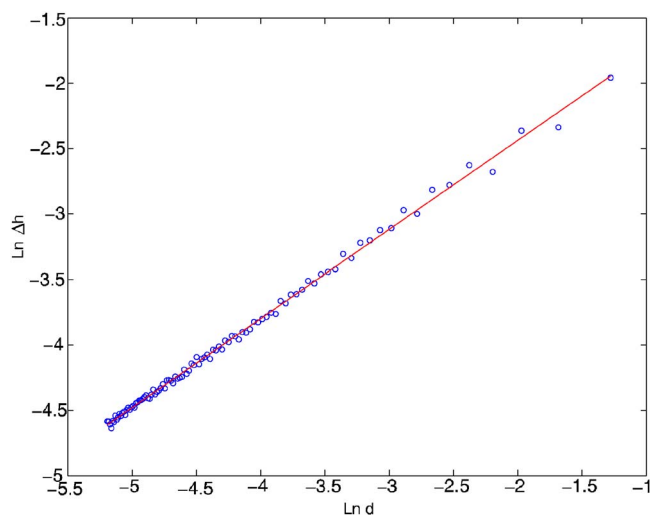


FIG. 17. (Color online) Roughness Δh of a single crack profile depending on window width d for one lattice of linear size $L = 100$; the position of the crack has in this case been determined by horizontal damage averaging (see text). The corresponding roughness exponent ζ is equal to 0.68.

For the considered case of strong disorder damage develops in three different stages. Initially some short-range localized growth of small fractures occurs, but this damage nucleates throughout the sample, due to the disorder. In the second stage the effect of disorder takes over and progression of the distributed damage follows a percolationlike picture, with random coalescence of different damage clusters. Already before the point of maximum stress macroscopic localization sets in, with a rough final crack preferentially growing in the direction perpendicular to the loading.

Numerical analysis shows that the macroscopic break-up mechanics and survival-probability statistics allow a power-law fitting of their size dependence; however, the power-law exponents are clearly different from those of random percolation. Such a macroscopic break-up analysis ignores the different mechanisms of damage development in the different stages before break-up, so no further interpretation on the deviating power-law fits can yet be drawn in terms of scaling; the latter may also be approximate and accidental. However, the microscopic data from the intermediate stage, with distributed development of damage, can clearly be fitted consistent with the theory of random percolation and with the theoretical values of its scaling exponents. This applies both to the damage-cluster mass statistics and to the spatial cluster extent. Surprisingly enough, scaling is still present in the last regime of damage development although the damage pattern is then strongly localized and anisotropic. Power-law dependence is followed very nicely by the crack roughness. The scaling of crack roughness is observed over more than three decades in lengthscale, only limited by the maximum size of

the lattice. When the final crack is identified by averaging the damage in the fracture cluster in the loading direction, the obtained value $\zeta = 0.65 \pm 0.07$ for the roughness-scaling exponent is consistent with the value 0.68 ± 0.04 that was determined experimentally for quasi-two-dimensional cracks in wood,²² with the result 0.71 ± 0.10 of numerical simulations for 2D graphite,²³ and marginally consistent with the prediction for random percolation in a gradient $\zeta = 8/11 = 0.73$.⁶ When alternatively the large-scale roughness is determined from the backbone of the infinite cluster, a roughness exponent $\zeta = 0.74 \pm 0.11$ is obtained; this is statistically sufficiently close to our averaging value. One may speculate that the agreement with the gradient-percolation value $\zeta = 8/11$ is due to the fact that the average position of the developing crack in the direction of load has already been largely frozen in around the maximum-stress point, and that further crack development is dominated by growth and coalescence in the transversal direction.

Our results may be compared with earlier simulation studies which consider fracture vs percolation. The results partially confirm those of Arbabi and Sahimi,¹² who used 2D triangular networks with the same type of power-law disorder, however, with bond-bending forces included and with disorder exponents $\alpha = 0.8$ and 0; they identified the percolationlike regime as the first regime of damage development, but based their conclusions on a graphical comparison of the force distribution in the network only, and did not give a more detailed quantitative analysis. When compared with the burning of fuse networks^{6,8} our investigation provides a more realistic model for the mechanics of fracture, as does the analysis of spring networks in Ref. 9. The percolationlike picture advocated in Ref. 6 is microscopically recognized in the present work, although only in a middle regime between the initial short-range and final long-range localization. Our data are not inconsistent with Refs. 8 and 9 either, but those studies do not analyze microscopic percolationlike behavior before the maximum stress, and concentrate on the final-stage scaling of the avalanchelike breakdown. Microscopic analysis of the localization regime in our model, and of the systematic damage-pattern variation with varying disorder exponent, will be the subject of future papers.

ACKNOWLEDGMENTS

This work is a part of the research programme of the Stichting voor Fundamenteel Onderzoek der Materie (FOM), which is financially supported by the Nederlandse Organisatie voor Wetenschappelijk Onderzoek (NWO). The computer facilities for this research were provided by Stichting Nationale Computerfaciliteiten (NCF). We thank E. van der Giessen (University of Groningen, RuG) and A. Hansen (Norwegian University of Science and Technology, NTNU) for stimulating discussions.

*Electronic address: i.malakhovsky@tue.nl

†Also at the Dutch Polymer Institute, www.polymers.nl

- ¹Z. P. Bažant, Arch. Appl. Mech. **69**, 703 (1999).
- ²W. Weibull, *Proceedings of Royal Swedish Institute for Engineering Research* (Ingenjörers Vetenskaps Akademiens, Handlingar, 1939), Vol. 153, pp. 1–55.
- ³S. Morel, E. Bouchaud, J. Schmittbuhl, and G. Valentin, Int. J. Fract. **114**, 307 (2002).
- ⁴C. S. Chang, T. K. Wang, L. J. Sluys, and J. G. M. van Mier, Eng. Fract. Mech. **69**, 1941 (2002).
- ⁵C. S. Chang, T. K. Wang, L. J. Sluys, and J. G. M. van Mier, Eng. Fract. Mech. **69**, 1959 (2002).
- ⁶A. Hansen and J. Schmittbuhl, Phys. Rev. Lett. **90**, 045504 (2003).
- ⁷H. J. Herrmann, A. Hansen, and S. Roux, Phys. Rev. B **39**, 637 (1989).
- ⁸P. K. V. V. Nukala, S. Šimunović, and S. Zapperi, J. Stat. Mech.: Theory Exp. 2004 P08001, 1–23.
- ⁹Phani Kumar V. V. Nukala, S. Zapperi, and S. Šimunović, Phys. Rev. E **71**, 066106 (2005).
- ¹⁰M. Sahimi, *Heterogeneous Materials I. Linear Transport and Optical Properties* (Springer-Verlag, New York, 2003).
- ¹¹M. Sahimi, *Heterogeneous Materials II. Nonlinear and Break-down Properties and Atomistic Modelling* (Springer-Verlag, New York, 2003).
- ¹²M. Sahimi and S. Arbabi, Phys. Rev. B **47**, 713 (1993).
- ¹³M. Sahimi and S. Arbabi, Phys. Rev. B **47**, 703 (1993).
- ¹⁴S. Arbabi and M. Sahimi, Phys. Rev. B **47**, 695 (1993).
- ¹⁵E. Schlangen and E. J. Garboczi, Int. J. Eng. Sci. **34**, 1131 (1996).
- ¹⁶S. Roux, A. Hansen, H. J. Herrmann, and E. Guyon, J. Stat. Phys. **52**, 237 (1988).
- ¹⁷D. Stauffer and A. Aharony, *Introduction to Percolation Theory* 2nd ed. (Taylor and Francis, London, 1992).
- ¹⁸H.-P. Hsu and M.-C. Huang, Phys. Rev. E **60**, 6361 (1999).
- ¹⁹R. Riedinger, M. Habar, P. Oelhafen, and H. J. Güntherodt, J. Comput. Phys. **74**, 61 (1988).
- ²⁰G. Grimmett, *Percolation* (Springer-Verlag, New York, 1989).
- ²¹H. J. Herrmann, D. C. Hong, and H. E. Stanley, J. Phys. A **17**, L261 (1984).
- ²²T. Engøy, K. J. Maløy, A. Hansen, and S. Roux, Phys. Rev. Lett. **73**, 834 (1994).
- ²³A. Omeltchenko, J. Yu, R. K. Kalia, and P. Vashishta, Phys. Rev. Lett. **78**, 2148 (1997).